Observations of the Optical Afterglow of GRB 050319 : Wind to ISM transition in view

Atish Kamble[1], L. Resmi[1,2], Kuntal Misra[3]

1. Introduction

One of the long standing questions in astrophysics is the progenitors of Gamma Ray Bursts (GRBs). Collapse of a massive star is one of the most favoured progenitors of the long GRBs. Evidence for a massive star being a GRB progenitor may be obtained in two different ways, both using observations of GRB afterglows. *(1) Supernova (SN) component underlying the GRB afterglow* : A few of the nearby GRB afterglows have shown the temporal and spectroscopic signature of an underlying SN. see e.g., (Stanek et al. 2003) *(2) Evolution of GRB afterglow in the stellar wind medium* : Massive stars modify the density profile of the circum-stellar medium due to the powerful winds they drive during their life time. For a constant mass loss rate and constant wind velocity the circum-burst medium assumes a density profile $\rho \propto r^{-2}$ as compared to $\rho =$ constant in the absence of stellar wind. Evolution of the GRB afterglow light curves is significantly different in these two cases of density profiles (Wijers and Galama 1999; Chevalier and Li 2000). Attempts to look for the signatures of such a wind-modified circum-burst density profile in the light curves of GRB afterglows have not been conclusive so far. In the case of GRB 050904 Gendre et al. (2007) finds that the early x-ray afterglow suggests a wind like density profile of the circum-burst medium while the late optical afterglow was consistent with evolution in a constant density medium. Hence, they conjecture that a transition between these two types of density profiles would have taken place somewhere in between. However, this transition was not directly observed in the light curve of any given band. We show that the afterglow of GRB 050319 could be explained as being due to the transition of the circum-burst density profile from wind-like to constant density.

GRB 050319 was detected by the Burst Alert Telescope (BAT) instrument of the SWIFT satellite on 2005 March 19, 09:31:18.44 UT (Krimm et al. 2005a,b). However,

[1]Raman Research Institute, Bangalore - 560 080, India

[2]Joint Astronomy Programme, Indian Institute of Science, Bangalore - 560 012, India

[3]Aryabhatta Research Institute of Observational Sciences, Manora Peak, Nainital - 263 129, India

Cusumano et al. (2006), using the re-analysis of the BAT data, pointed out that *Swift* was slewing during the GRB onset and the BAT trigger was switched off. The GRB was recognised about 135 seconds after its actual onset. The total duration of the GRB (T_{90}) was thus 149.7 s (Cusumano et al. 2006) instead of 10 ± 2 s (Krimm et al. 2005a,b). The burst fluence in 15-350 keV band within the T_{90} duration is estimated to be 1.6×10^{-6} erg cm^{-2}. The photon index of the time-averaged single power law spectrum is 2.1 ± 0.2. *Swift* XRT and UVOT located a bright source at $\alpha = 10^{h}16^{m}48^{s}$ and $\delta = +43°32'47''$ (J2000) which was later confirmed by Rykoff et al. (2005) with ROTSE-IIIb. Fynbo et al. (2005) obtained the spectra of the afterglow of GRB 050319 on 2005 March 20 and the redshift of the afterglow was measured to be z = 3.24. At this redshift, the gamma ray isotropic equivalent energy released during the burst is 3.7×10^{52} erg for a flat universe with $\Omega_m = 0.3, \Omega_\Lambda = 0.7$ and $H_0 = 70$ km s^{-1} Mpc^{-1}.

2. Observations and Data Reduction

Optical CCD observations of the afterglow of GRB 050319 were carried out in Johnson BV and Cousins RI filters using the 104-cm Sampurnanand Telescope of ARIES, Nainital with regular specifications of the CCD camera and using standard observation procedures of bias subtraction and flat fielding. For details see Misra et al. (2007).

The BVRI magnitudes of the optical transient (OT) obtained were calibrated differentially using secondary stars numbered 8, 9, 10, 11 and 13 in the list of Henden (2005). The magnitudes derived in this way are given in Table 1. Photometric magnitudes available in the literature by Woźniak et al. (2005); Quimby et al. (2006); Mason et al. (2006); Huang et al. (2007) were converted to the present photometric scales using the five secondary stars mentioned above.

3. Light curves of GRB 050319

Along with our own observations we have used observations reported in the literature to study the light curves of GRB 050319 afterglow. The x-ray afterglow was observed by *Swift* XRT starting from $\sim$ 220s to 28 days (Cusumano et al. 2006) after the burst. Attempts to observe the afterglow at radio wavebands resulted in upper limits (Soderberg 2005a,b; Volvach and Pozanenko 2005). The optical afterglow was observed by Woźniak et al. (2005); Quimby et al. (2006); Mason et al. (2006) resulting in a coverage from a few seconds to ~ 4

Date (UT) 2005 March	Magnitude (mag)	Exposure Time (s)	Passband
19.7512	21.02±0.14	2×900	B
19.7457	20.23±0.20	600	V
19.8558	20.60±0.21	600	V
19.6949	19.46±0.16	300	R
19.6999	19.25±0.10	300	R
19.7215	19.98±0.11	300	R
19.7539	20.06±0.13	300	R
19.7874	20.03±0.16	300	R
19.7129	19.59±0.19	300	I
19.7587	19.66±0.25	300	I

Table 1: CCD BVRI broad band optical observations of the GRB 050319 afterglow using the 104-cm Sampurnanand Telescope at ARIES, Nainital.

days after the burst.

To construct the optical light curve we have corrected the observed magnitudes for the standard Galactic extinction law given by Mathis (1990). The galactic extinction in the direction of GRB 050319 is estimated to be E(B-V) = 0.011 mag from the smoothed reddening map provided by Schlegel et al. (1998). The effective wavelength and normalization given by Bessell et al. (1998) were used to convert the magnitudes to fluxes in μJy.

Most of the GRB afterglow light curves are well characterized by a broken power law of the form $F = F_0\{(t/t_b)^{\alpha_1 s} + (t/t_b)^{\alpha_2 s}\}^{-1/s}$ where α_1 and α_2 are the afterglow flux decay indices before and after the break time (t_b), respectively. F_0 is the flux normalization and 's' is a smoothening parameter which controls the sharpness of the break. Most known GRB afterglows have $\alpha_2 > \alpha_1$ i.e. the decay becomes steeper after the break. Interestingly, the optical afterglow light curve of GRB 050319 shows steeper to flatter decay with a break at ~ 0.02 day. This behavior of light curve decay is difficult to explain within the standard afterglow models. The x-ray and optical light curves also show some variability superimposed

on the power law decay. The x-ray light curve shows a break near ~ 0.3 day. We quantify the various characteristics of the afterglow light curves as summarized below.

1. The x-ray afterglow of GRB 050319 shows a very rapid decay before ~ 0.005 day (~ 384 s) after the GRB. The decay then flattens before steepening again at ~ 0.3 day. Cusumano et al. (2006) has characterised the afterglow into three separate temporal evolutions in x-ray bands : $\alpha_{\rm X1} = 5.53 \pm 0.67$ (Δt < 384 s); $\alpha_{\rm X2} = 0.54 \pm 0.04$ (384 s $< \Delta$t < 0.3day); $\alpha_{\rm X3} = 1.14 \pm 0.2$ (Δt > 0.3day);

2. The B, V and R band light curve also show a rapid decline during the early phase (Δt < 0.02 day) which flattens at later epochs. Thus, the afterglow can be separated into two separate temporal evolutions in R band $\alpha_{\rm R1} = 1.09 \pm 0.03$ (Δt < 0.02day); $\alpha_{\rm R2} = 0.51 \pm 0.03$ (0.02day $< \Delta$t < 10.0day);
And for B, V and I bands we measure following α s : $\alpha_{\rm B1} = 1.46 \pm 0.26$ (Δt < 0.02day); $\alpha_{\rm B2} = 0.33 \pm 0.05$ (0.02day $< \Delta$t < 1.0day); $\alpha_{\rm V1} = 0.90 \pm 0.05$ (Δt < 0.02day); $\alpha_{\rm V2} = 0.50 \pm 0.04$ (0.02day $< \Delta$t < 1.0day); $\alpha_{\rm I2} = 0.59 \pm 0.13$ (0.02day $< \Delta$t < 1.0day); The average decay index of the optical light curve, at early and late epochs, is then 1.15 ± 0.27 and 0.48 ± 0.15 respectively.

4. GRB 050319 afterglow : wind or homogeneous density profile ?

The breaks seen in x-ray light curve (at ~ 384 s and at ~ 0.3 day) are not accompanied by simultaneous breaks in optical wavebands. Similarly, the break seen in optical band has no simultaneous counterpart in the x-ray light curve. Also, the sense of slope change, i.e. $\alpha_2 < \alpha_1$, as seen in optical waveband is contrary to the predictions of the fireball model (Sari et al. 1998, 1996) which expects $\alpha_1 < \alpha_2$.

We propose a different model to explain the afterglow of GRB 050319 as being due to a transition of the circum-burst medium density profile that the explosion generated shock wave is interacting with. We propose that the observed change from steep to flat decay of the optical afterglow of GRB 050319 at 0.02 day is due to the change in the density profile of the circum-burst medium from wind modified ($\rho \propto r^{-2}$) to the constant density medium (ρ = constant). The break in the light curve occurs when the shock front interacts with the boundary between the two density profiles. Below we describe and reproduce various features of the GRB 050319 afterglow using this model of 'wind to constant density medium transition'.

The early steep decay of x-ray afterglows ($\alpha \sim 3$ to 5) as is seen in the case of GRB 050319 are now seen routinely in most of the GRBs (Nousek et al. 2006) and has become a canonical feature of the GRB x-ray afterglows. In the case of GRB 050319 Cusumano et al. (2006) conjecture that the early steep decay emission could be low energy tail of the GRB prompt emission. We exclude this early emission from the rest of our discussion and we will restrict ourselves to the rest of the x-ray light curve.

The radiation spectrum of GRB afterglows exhibits a power law spectrum characterised by three break frequencies - the self absorption frequency $\nu_{\rm a}$, the peak frequency $\nu_{\rm m}$ corresponding to the lower cutoff in the electron energy distribution ($n(\gamma) \propto \gamma^{-p}$, $\gamma > \gamma_m$), and the synchrotron cooling frequency $\nu_{\rm c}$. The flux $F_{\rm m}$ at $\nu_{\rm m}$ provides the normalisation of the spectrum (Sari et al. 1998).

The photon index (Γ) of the afterglow and the electron energy distribution index p are related in any given spectral regime ($\Gamma - 1 = p/2$ if $\nu_{\rm c} < \nu$ and $\Gamma - 1 = (p-1)/2$ if $\nu < \nu_{\rm c}$). The corresponding temporal decay index α would be $(3p-2)/4$ and $3(p-1)/4$ respectively before the jet break and would equal p in both spectral regimes after the jet break, according to the standard fireball model for an afterglow expanding in a homogeneous interstellar medium (ISM). For the shock wave expanding into the wind density profile the corresponding α would be $(3p-2)/4$ and $(3p-1)/4$ respectively before the jet break and p after the jet break.

In the present case, the observed values of the photon index ($\Gamma = 1.69 \pm 0.06$) and temporal decay index ($\alpha_{\rm X} = 0.54 \pm 0.04$) of the x-ray afterglow are consistent with the spectral regime $\nu_{\rm X} > \nu_{\rm c}$ and $p = 1.5$. The observed decay indices of optical light curve are also consistent with the inferred value of p, the spectral regime $\nu_{\rm opt} < \nu_{\rm c}$ and wind-constant density transition at 0.02 day. As discussed above, the expected temporal decay index of the x-ray afterglow, $\alpha_{\rm X} = (3p-2)/4$, is the same for wind and homogeneous ISM density profiles. The absence of a break in the x-ray afterglow light curve simultaneous with the optical break makes the multiband afterglow features consistent with the proposed transition of the circum-burst medium density profile from wind to constant density. In Figure 1. we compare the predictions of our model of wind to constant density transition of the circum-burst density profile with multiband observations of GRB 050319 afterglow. A detailed list of the best fit spectral parameters can be found in Table 2. The observed B band light curve is systematically lower than that predicted by the model which could be due to the *Lyman* α absorption at $z = 3.24$ appearing in the observer's B band as suggested by Huang et al. (2007). The steepening of the x-ray light curve at $\Delta t \sim 0.3$ day could be due to jet break (Cusumano et al. 2006) but unfortunately the variability in R band light curve and insufficient sampling of the data in B and V bands after ~ 1.0 day makes it difficult to

verify the achromaticity of the break.

Given the above model spectral parameters we find that the broadband behavior of the afterglow is very well explained. However, we are restricting ourselves to the overall behavior of the afterglow and hence do not attempt in our model to reproduce the variations seen in the optical light curve. The reason for these variations could be density inhomogenities in the circum-burst medium.

4.1. Physical Parameters

Four spectral parameters ($\nu_{\rm a}, \nu_{\rm m}, \nu_{\rm c}$ and $\rm F_{peak}$) are related to four physical parameters viz n (no density of the constant density circum-burst medium) or A_* (defined as $\rho(r) = 5 \times 10^{11} A_* r^{-2}$ for wind density medium), E (total energy content of the fireball), energy fraction in relativistic electrons $\epsilon_{\rm e}$ and that in magnetic field ϵ_B. The typical value of self absorption frequency $\nu_{\rm a}$ lies in radio-mm waves and hence is best estimated only if the afterglow is well observed in these bands. Unfortunately, the afterglow of GRB 050319 was never detected at the radio band (Soderberg 2005a,b; Volvach and Pozanenko 2005). Therefore we expressed the remaining three spectral parameters, known separately from parts of the light curves corresponding to the wind and the constant density circum-burst medium, in terms of $\rm A_*$ and n, respectively. Equating the kinetic energies estimated from two density profiles, i.e. $E^K_{wind} = E^K_{ISM}$, we obtain a relation between $\rm A_*$ and n : $\rm A_* = 5.097 \times 10^{-3}\ n^{2/5}$. For a typical range of values of n (1 to 100), estimated $\rm A_*$ ranges from 5.097×10^{-3} to 0.032 which results in the range of E^K_{iso} from 1.3×10^{54} to 5.3×10^{53} erg. All the estimated physical parameters are listed in Table 3.

5. Discussion

5.1. Signature of Wind Reverse Shock ?

Morphology and evolution of the wind bubbles has been studied by Castor et al. (1975); Weaver et al. (1977). A reverse shock forms at the surface where the stellar wind meets the surrounding ISM and it then propagates into the wind. The free wind (upstream of the reverse shock) has a density profile $\rho \propto r^{-2}$ and the shocked wind (downstream of the reverse shock) has a constant density profile. The effects of such a density transition on the afterglow of a GRB has been studied by Pe'er and Wijers (2006). It could be this transition of the density profile that we are observing at 0.02 day in the present case of GRB 050319. From

the observations of long GRB afterglows, it has been inferred that most of the GRBs occur in constant density environment and the absence of wind signatures in the GRB afterglow was surprising. Various ways which can bring the wind reverse shock closer to the exploding star have recently been proposed to resolve this mystery surrounding the absence of winds (van Marle et al. 2006; Eldridge 2007). In the case of GRB 050319, for a range of assumed values of $n = 1$ *to* 100 we estimate the radius of the reverse shock to be $R_{SW} \sim 0.5$ pc to 0.1 pc comparable to the values obtained by Eldridge (2006). The constraint $\epsilon_B < 1$ puts a lower bound on density : $n > 0.03$

5.2. Implications for the models of GRB progenitors

Our interpretation of the afterglow of GRB 050319 as being due to the wind-constant density transition supports the collapsar model of GRBs. Detection of similar transitions in other afterglows have so far eluded us perhaps because of the smaller size of the wind bubbles and the resultant early transition times. The present detection was made possible chiefly because of the quick follow up abilities of the robotic telescopes RAPTOR (Woźniak et al. 2005) and ROTSE-III (Quimby et al. 2006) coupled with those of *Swift* XRT (Cusumano et al. 2006) and UVOT (Mason et al. 2006). Time dilation due to cosmological redshift delays the occurrence of the transition in the observer's frame of reference and makes it favourable to detect such a transition in distant GRBs. The robotic telescopes are now routinely detecting GRB afterglows as early as a few minutes after the burst and with careful analysis of multiband observations of distant GRBs it should be possible to detect more examples of similar transition. For example, a probable detection of similar density transition, though not in the same waveband, has been reported by Gendre et al. (2007) in the case of GRB 050904 (z $\sim$ 6.3) where the transition time is assumed to be $\sim$ 1700 s ($\sim$ 0.02 days) after the burst, similar to that for GRB 050319 afterglow in the present case.

6. Summary

We have modeled the multiband afterglow of GRB 050319, using our own optical observations and other observations available in the literature, as being due to the interaction of the relativistic blast wave with circum-burst medium which shows a transition of density profile from wind to constant density. Our conclusions can be summarised as follows :

1. We present BVRI band observations of GRB 050319 afterglow.

2. We showed that the unusual break in the light curves of optical afterglow at 0.02

day can be explained as being due to the transition of circum-burst density profile from wind to constant density. The observed x-ray afterglow light curve without a simultaneous break is consistent with this interpretation. The overall afterglow can be explained by using a relatively low value of electron energy distribution index p which is also consistent with the x-ray spectral photon index.

3. The transition of the density profile could be due to the wind reverse shock propagating into the stellar wind driven by the progenitor of GRB 050319. We estimate radius of the wind reverse shock to be $R_{SW} \sim 0.5\ pc\ to\ 0.1\ pc$ for assumed values of $n \sim 1\ to\ 100$ cm^{-3} respectively.

Acknowledgments

We are thankful to D. Bhattacharya for critical comments and detailed discussions throughout this work and to Ram Sagar for his support during the observations. We are thankful to the anonymous referee for constructive comments which has improved the *Letter* significantly.

REFERENCES

K. Z. Stanek, T. Matheson, P. M. Garnavich, P. Martini, P. Berlind, N. Caldwell, P. Challis, W. R. Brown, R. Schild, K. Krisciunas, et al., ApJ Lett **591**, L17 (2003), `astro-ph/0304173`.

R. A. M. J. Wijers and T. J. Galama, ApJ **523**, 177 (1999), `astro-ph/9805341`.

	wind density medium	constant density medium
$\nu_m(Hz)$	$1.6^{+0.9}_{-0.7} \times 10^{13}$	$1.0^{+0.35}_{-0.5} \times 10^{12}$
$\nu_c(Hz)$	$1.1^{+3.7}_{-0.4} \times 10^{15}$	$2.1^{+0.6}_{-0.8} \times 10^{15}$
$F_{peak}(\mu Jy)$	2370 ± 355	1810^{+260}_{-170}
p	1.59 ± 0.06	1.52 ± 0.02
$\chi^2_{dof}(dof)$	1.4 (161)	

Table 2: The best fit spectral parameters for wind (< 0.02 day) and constant density (> 0.02 day) profile. All the parameters are fitted at 0.003 day after the burst.

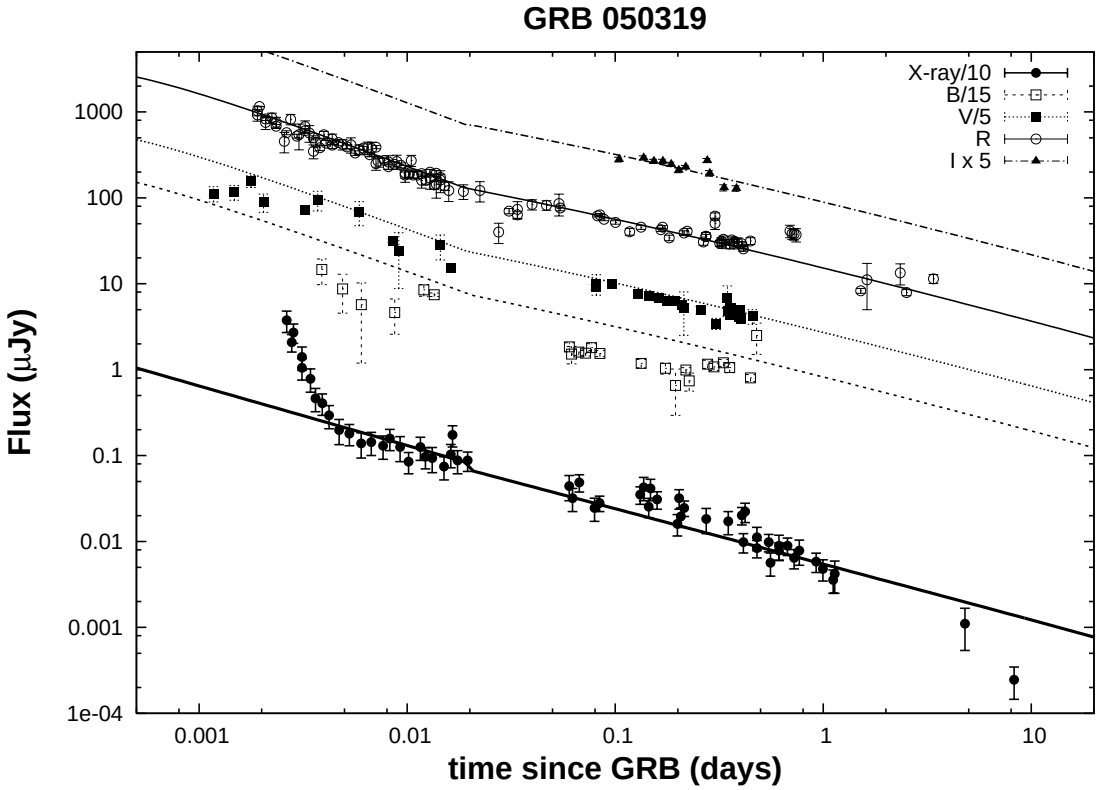

Fig. 1.— The afterglow light curves of GRB 050319. The solid lines represent a model in which the expanding fireball encounters the transition in density profile from the wind to constant density medium at 0.02 day. The best fit spectral parameters of this model are listed in Table 2

Parameter	n = 1; $A_* = 5.097 \times 10^{-3}$		n = 100; $A_* = 0.032$	
	wind	ISM	wind	ISM
E_{54}^{iso}	1.3	1.3	0.53	0.53
ϵ_e	4.4×10^{-3}	2.2×10^{-3}	1.1×10^{-2}	5.4×10^{-3}
ϵ_B	0.14	1.2×10^{-3}	0.01	$\sim 10^{-4}$

Table 3: Physical parameters estimated using the best fit spectral parameters mentioned in Table 2

R. A. Chevalier and Z.-Y. Li, ApJ **536**, 195 (2000), astro-ph/9908272.

B. Gendre, A. Galli, A. Corsi, A. Klotz, L. Piro, G. Stratta, M. Boër, and Y. Damerdji, A&A **462**, 565 (2007), astro-ph/0603431.

H. Krimm, M. Still, S. Barthelmy, L. Barbier, S. Campana, M. Capalbi, M. Chester, J. Cummings, E. Fenimore, N. Gehrels, et al., GRB Coordinates Network **3117**, 1 (2005a).

H. Krimm, T. Sakamoto, S. Barthelmy, L. Barbier, J. Cummings, E. Fenimore, N. Gehrels, D. Hullinger, C. Markwardt, F. Marshall, et al., GRB Coordinates Network **3119**, 1 (2005b).

G. Cusumano, V. Mangano, L. Angelini, S. Barthelmy, A. P. Beardmore, D. N. Burrows, S. Campana, J. K. Cannizzo, M. Capalbi, G. Chincarini, et al., ApJ **639**, 316 (2006), 2005astro.ph..9689C.

E. Rykoff, B. Schaefer, and R. Quimby, GRB Coordinates Network **3116**, 1 (2005).

J. P. U. Fynbo, J. Hjorth, B. L. Jensen, P. Jakobsson, P. Moller, and J. Naranen, GRB Coordinates Network **3136**, 1 (2005).

K. Misra, D. Bhattacharya, D. K. Sahu, R. Sagar, G. C. Anupama, A. J. Castro-Tirado, S. S. Guziy, and B. C. Bhatt, ArXiv Astrophysics e-prints (2007), astro-ph/0701413.

A. Henden, GRB Coordinates Network **3454**, 1 (2005).

P. R. Woźniak, W. T. Vestrand, J. A. Wren, R. R. White, S. M. Evans, and D. Casperson, ApJ Lett **627**, L13 (2005), astro-ph/0505336.

R. M. Quimby, E. S. Rykoff, S. A. Yost, F. Aharonian, C. W. Akerlof, K. Alatalo, M. C. B. Ashley, E. Göğüş, T. Güver, D. Horns, et al., ApJ **640**, 402 (2006), 2005astro.ph.11421Q.

K. O. Mason, A. J. Blustin, P. Boyd, S. T. Holland, M. J. Page, P. Roming, M. Still, B. Zhang, A. Breeveld, M. de Pasquale, et al., ApJ **639**, 311 (2006), astro-ph/0511132.

K. Y. Huang, Y. Urata, P. H. Kuo, W. H. Ip, K. Ioka, T. Aoki, C. W. Chen, W. P. Chen, M. Isogai, H. C. Lin, et al., ApJ Lett **654**, L25 (2007), astro-ph/0611323.

A. M. Soderberg, GRB Coordinates Network **3127**, 1 (2005a).

A. M. Soderberg, GRB Coordinates Network **3132**, 1 (2005b).

A. Volvach and A. Pozanenko, GRB Coordinates Network **3153**, 1 (2005).

J. S. Mathis, ARA&A **28**, 37 (1990).

D. J. Schlegel, D. P. Finkbeiner, and M. Davis, ApJ **500**, 525 (1998), astro-ph/9710327.

M. S. Bessell, F. Castelli, and B. Plez, A&A **333**, 231 (1998).

R. Sari, T. Piran, and R. Narayan, ApJ Lett **497**, L17+ (1998), astro-ph/9712005.

R. Sari, R. Narayan, and T. Piran, ApJ **473**, 204 (1996), astro-ph/9605005.

J. A. Nousek, C. Kouveliotou, D. Grupe, K. L. Page, J. Granot, E. Ramirez-Ruiz, S. K. Patel, D. N. Burrows, V. Mangano, S. Barthelmy, et al., ApJ **642**, 389 (2006), astro-ph/0508332.

J. Castor, R. McCray, and R. Weaver, ApJ Lett **200**, L107 (1975).

R. Weaver, R. McCray, J. Castor, P. Shapiro, and R. Moore, ApJ **218**, 377 (1977).

A. Pe'er and R. A. M. J. Wijers, ApJ **643**, 1036 (2006), astro-ph/0511508.

A. J. van Marle, N. Langer, A. Achterberg, and G. Garcaía-Segura, A&A **460**, 105 (2006), astro-ph/0605698.

J. J. Eldridge, ArXiv Astrophysics e-prints (2007), astro-ph/0701707.

J. J. Eldridge, ArXiv Astrophysics e-prints (2006), astro-ph/0610413.